3 Biotech (2017) 7:238
DOI 10.1007/s13205-017-0861-z

ORIGINAL ARTICLE

Zinc oxide–curcumin nanocomposite loaded collagen membrane as an effective material against methicillin-resistant coagulase-negative Staphylococci

K. R. Soumya[1] · S. Snigdha[3] · Sheela Sugathan[2] · Jyothis Mathew[1] · E. K. Radhakrishnan[1]

Received: 19 June 2017 / Accepted: 22 June 2017 / Published online: 11 July 2017

Abstract Zinc oxide nanoparticles and curcumin are excellent antimicrobial agents. They have the potential to be used as alternative to antibiotics in wound infection management. In this study, ZnO–curcumin nanocomposite was synthesized and characterized. Physical adsorption of the nanocomposite onto collagen skin wound dressing was conducted and structural investigation was carried out by SEM. Antimicrobial assay, minimum inhibitory concentration (MIC), and viability assays of different concentrations of nanocomposite loaded collagen membrane were conducted against clinically isolated methicillin-resistant coagulase-negative Staphylococci (MRCoNS), such as *S. epidermidis*, *S. hemolyticus,* and *S. saprophyticus*. The nanocomposite showed excellent anti-CoNS activity on time kill assay with the MIC value of 195 µg/mL against *S. epidermidis*, *S. hemolyticus* and 390 µg/mL against *S. saprophyticus*. The nanocomposite loaded collagen membrane also showed excellent in vitro antistaphylococcal activity. This study may lead to the development of antibiotic alternate strategies to control and limit the MRCoNS in wound-related infections.

Keywords Zinc oxide · Curcumin · Nanocomposite · Methicillin-resistant coagulase-negative Staphylococci · Antistaphylococcal

Introduction

Coagulase-negative Staphylococci (CoNS) are commensal bacteria which mainly include *Staphylococcus epidermidis*, *S. hemolyticus*, *S. saprophyticus,* and *S. hominis*. CoNS have been reported to be the major etiological agents in nosocomial infections of skin and soft tissues. The marked increase in the occurrence of drug-resistance genes among CoNS isolated from skin-related wounds and ulcers are alarming. Multidrug resistance and biofilm formation have been reported in large number of clinically isolated Staphylococci and this demands the development of alternative therapeutic strategies (Piette and Verschraegen 2009).

Nanoparticles, phytochemicals, and their combinations have gained a lot of attention in wound healing applications. This is because of the low risk and multitargeted action of these antibiotic-alternatives (Tocco et al. 2012). The current study demonstrates the efficacy of zinc oxide nanoparticle–curcumin hybrid in inhibiting methicillin-resistant CoNS. ZnO nanoparticles have been found to be nontoxic to animals and also proved to be efficient antimicrobials (Jin et al. 2009). Curcumin has been studied extensively for its use as an anticancer, anti-inflammatory, antimicrobial, and anti-aging agent (Aggarwal et al. 2007; Mun et al. 2014). Both curcumin and ZnO are also known for their remarkable effects to accelerate wound healing

K. R. Soumya and S. Snigdha contributed equally.

Electronic supplementary material The online version of this article (doi:10.1007/s13205-017-0861-z) contains supplementary material, which is available to authorized users.

✉ E. K. Radhakrishnan
radhakrishnanek@mgu.ac.in

[1] School of Biosciences, Mahatma Gandhi University, PD Hills (PO), Kottayam, Kerala 686 560, India

[2] Sree Narayana Institute of Medical Sciences, Chalakka, Ernakulam, Kerala 683 594, India

[3] International and Inter University Centre for Nanoscience and Nanotechnology, Mahatma Gandhi University, PD Hills (PO), Kottayam, Kerala 686 560, India

through diverse mechanisms (Augustine et al. 2014; Mei et al. 2016; Mohanty et al. 2012; Panchatcharam et al. 2006). Hence, ZnO–curcumin nanocomposite can expect to have improved antimicrobial and wound healing properties.

In the present study, nanocomposite of zinc oxide nanoparticles and curcumin was prepared as an alternative to antibiotics. The nanocomposite was then loaded onto commercially available collagen wound dressing to improve the antimicrobial and wound healing effects. Along with the components of the nanocomposite prepared in the study, the collagen skin dressing is also known for its excellent stimulatory effect on new tissue growth, which makes the preparation developed in the study to have promising clinical applications. Hence, antistaphylococcal activity of zinc oxide–curcumin loaded collagen dressing demonstrated in this study confirms its feasibility as an alternative therapeutic agent and excellent skin-dressing material.

Materials and methods

MRCoNS collection

Three methicillin-resistant clinical isolates of CoNS were selected for this study. The selected isolates were *S. epidermidis* 107, *S. hemolyticus* 143, and *S. saprophyticus* 4 which were collected from a tertiary care hospital in Ernakulam, Kerala, India. These isolates were identified by biochemical tests using HiStaph Ident Kit (Himedia, Mumbai) and also by molecular methods as described in our previous study (Soumya et al. 2016). The selected isolates were also studied phenotypically and genotypically for methicillin resistance. The three cultures were made to culture stock of Molecular Microbiology Laboratory of School of Biosciences, Mahatma Gandhi University, Kottayam, Kerala, India under the numbers SBMML107, SBMML143, and SBMML4, respectively, for *S. epidermidis* 107, *S. hemolyticus* 143, and *S. saprophyticus* 4.

Antibacterial analysis of ZnO by well diffusion assay

Well diffusion tests were carried out to confirm the antibacterial activity of zinc oxide nanoparticles (DLS particle size <100, <35 nm, average particle size; 721,077, Sigma Aldrich, India) and curcumin (Kancor, Kerala) against *S. epidermidis* 107, *S. hemolyticus* 143, and *S. saprophyticus* 4. The isolates were inoculated in Mueller-Hinton Broth (MHB) (Himedia, Mumbai) and incubated at 37 °C for 24 h. The overnight cultures were diluted to 0.5 McFarland standard. Wells of 6 mm diameter were made on Mueller–Hinton agar (MHA) (Himedia, Mumbai) plates using a gel puncture. Furthermore, the selected isolates were spread plated on the surface of MHA plates. The zinc oxide nanoparticles were prepared at concentrations ranging from 75, 50, 25, 10, and 5 mg/mL in distilled water. Curcumin was prepared in concentrations ranging from 1000, 750, 500, and 250 μg/mL in methanol. From the various concentrations prepared, 50 μL was taken and was added to the wells prepared in the MHA plate. Methanol was used as control for curcumin antibacterial assay. The diameter of the zone of inhibition around each well was measured after incubation at 37 °C for 24 h. All the tests were performed in triplicates.

Synthesis of zinc oxide–curcumin (ZC) nanocomposite

Curcumin dissolved in methanol was added dropwise to aqueous ZnO nanoparticle suspension under constant sonication in a water bath sonicator at 50 kHz for 4 h. Zinc oxide nanoparticles and curcumin were taken in 1:1 ratio. After the completion of sonication, a change in color from yellow to orange was observed. This suspension was centrifuged and the supernatant was discarded. The pellet was dried at 40 °C to obtain a fine orange-colored powder (Dhivya et al. 2015).

Characterisation of ZC nanocomposite

The characterisation of ZnO nanoparticles, curcumin, and ZC nanocomposite was done by UV spectrophotometry, XRD, FTIR, and SEM analysis. UV–Visible absorbance spectra were recorded using Shimadzu UV 2600 plus spectrophotometer in the range of 300–600 nm at a resolution of 1 nm. X-ray diffraction patterns of ZnO nanoparticles, curcumin, and ZC nanocomposite were obtained with diffractometer model D8 Advance of Bruker (Germany) using Cu Kα (1.5406 Å) radiation operating with 30 mA and 45 kV in the 2θ range of 10°–90°. The Fourier transform infrared (FTIR) spectra were recorded using the KBr pellet technique in 500–4000 cm^{-1} frequency range (Shimadzu IR Prestige 21). Scanning electron microscopic images of finely powdered samples were obtained by JEOL JSM 6390 microscope.

MIC of nanocomposite against MRCoNS

The minimum inhibitory concentration (MIC) of ZC nanocomposite against *S. epidermidis* 107, *S. hemolyticus* 143, and *S. saprophyticus* 4 was determined by broth microdilution assay (CLSI 2013). The MHB cultures of three clinical isolates were incubated at 37 °C. The broth culture was adjusted with sterile saline to obtain turbidity comparable to that of 0.5 McFarland standard.

Nanocomposite was tested in triplicates at ten different double-diluted concentrations ranging from 6250 to 12 μg/mL. For this, CONS cultures were added to wells containing 100 μL of MHB and 100 μL of ZC nanocomposite and were incubated at 37 °C for overnight. MICs were recorded as the lowest concentration of nanocomposite that inhibited the visible growth of bacteria after 24 h incubation at 37 °C. The absorbance was recorded at 600 nm for each well using an ELISA reader (thermo varioskan multimode reader) and the results were compared to control without NC composite treatment.

Time kill assay and fluorescence microscopic analysis

Time kill assay was determined for the minimum inhibitory concentration of ZC nanocomposite against the three MRCoNS isolates. The 24 h bacterial cultures in MHB medium with turbidity comparable to 0.5 McFarland standard were incubated with their respective MIC concentrations of nanocomposite in a shaking incubator. From this, aliquots of samples were taken at 0, 4, 6, 8, and 24 h intervals and OD at 600 nm was measured. The time kill assay was performed in quadruplicate. Fluorescence microscopy was used for analysing the effect of nanocomposite on the viability of bacterial samples. Acridine orange was used to differentiate between the live and dead cells. After 24 h, samples were aliquoted, stained, and visualised as per previously reported method (Thomas et al. 2015).

Scanning electron microscopy of ZC treated and control samples of MRCoNS

Mid-log-phase CoNS cultures were treated overnight with 1 mg/mL of ZC nanocomposite. 10 μL each of treated and untreated bacterial suspensions were deposited on separate glass slides and dried. The dried samples were then fixed using a primary fixative solution containing 3% glutaraldehyde for 2 h, followed by dehydration with a series of ethanol solutions (50, 80, and 100%). Finally, the samples were mounted on SEM stubs and coated with platinum using a JEOL JFC 1600 Autofine coater. JEOL JSM 6390 scanning electron microscope operating at 10 kV was used to image the prepared samples.

Introduction of ZC nanocomposite into collagen skin wound dressing and in vitro analysis of antistaphylococcal activity

Different concentrations of ZC nanocomposite (1, 5, and 10 mg/mL) were dispersed in sterile water. The commercially available collagen skin wound dressing (Kollagen, Eucare pharmaceuticals Pvt Ltd, Chennai, India) was immersed in the nanocomposite solution for 24 h. The membrane was then washed in sterile saline and allowed to dry. The treated membrane with dimensions of 1 × 1 cm was used for further studies. Untreated membranes of identical dimensions were used as control. Overnight culture of MRCoNS was spread on MHA plates and prepared collagen membranes were placed over the microbial lawn. After incubation at 37 °C for 24 h, zone of clearance around the collagen sections was recorded. These membranes were dried, sectioned, and mounted onto SEM grid. Samples were sputter coated with platinum and examined using JEOL JSM 6390 scanning electron microscope at 10 kV.

Results

Antibacterial activity of ZnO nanoparticles and curcumin against MRCoNS

Antibacterial activity of zinc oxide NPs and curcumin against *S. epidermidis* 107, *S. hemolyticus* 143, and *S. saprophyticus* 4 was done using well diffusion assay. Zinc oxide NPs and curcumin showed antimicrobial activity for all the tested concentrations (Supplementary Fig. 1). Zone of inhibition recorded is given in Supplementary Table 1.

Synthesis and characterization of zinc oxide–curcumin nanocomposite

Synthesis of the ZC nanocomposite was conducted under constant sonication for 4 h and color change of reaction mixture from yellow to orangish red indicated the formation of ZC nanocomposite (Supplementary Fig. 2). The UV–Visible absorption spectra of the nanoparticles are illustrated in Fig. 1a.

ZnO NPs and curcumin exhibited their characteristic strong absorption bands at 360 and 420 nm, respectively. In ZC nanocomposites, two absorption bands at 319 and 438 nm were observed. The curcumin absorption peak (424 nm) experienced a red shift to 438 nm. The band shifts observed in nanocomposite from their corresponding parental components clearly indicate an interaction between the two components and formation of stable nanocomposite (Dhivya et al. 2015). The FTIR spectrum of the ZnO nanoparticles, curcumin, and ZC nanocomposite was scanned in the range of 500–4000 cm^{-1}. The peak at 667 cm^{-1} is representative of Zn–O stretching vibrations of ZnO nanoparticles. The peaks at 802, 833, and 881 cm^{-1} are characteristic absorption bands of metal oxides due to inter atomic vibrations. The peaks at 1197 and 3346 cm^{-1} may be due

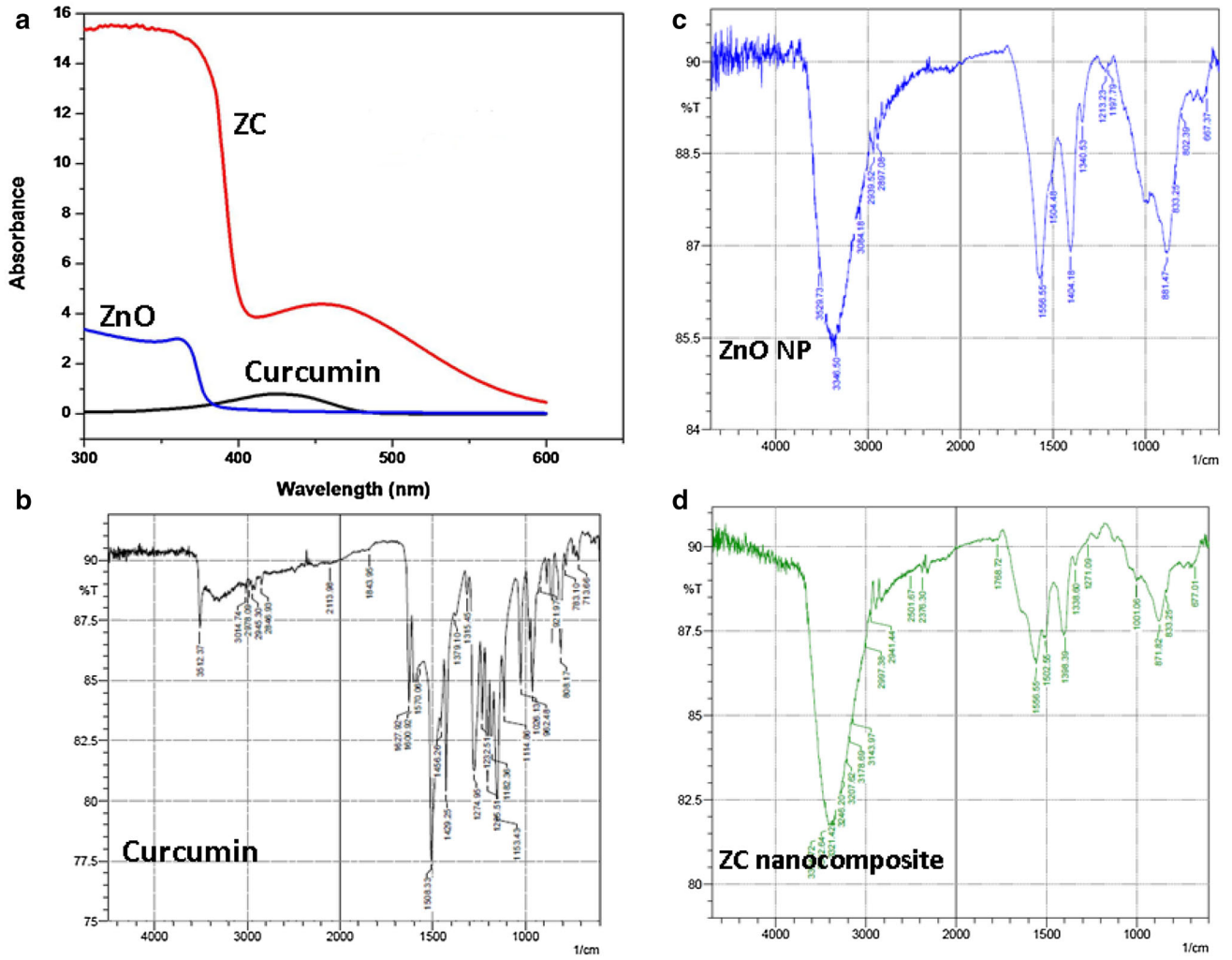

Fig. 1 **a** UV–Visible spectrum of ZnO nanoparticles (ZnO), curcumin, and zinc oxide–curcumin nanocomposite (ZC); FTIR spectra of **b** curcumin, **c** ZnO nanoparticles, and **d** ZnO–curcumin nanocomposite

to –OH deformation and stretching, respectively, on account of the moisture adsorbed on the NP surface (Kumar and Rani 2013). The FTIR spectra of curcumin produced a characteristic stretching band of O–H at 3512 cm^{-1}. The peak at 3014 cm^{-1} pertains to C–H stretching and 1600 cm^{-1} peak represents C=C symmetric aromatic ring stretching. The peak at 1508 cm^{-1} is for C=O, while enol C–O peak was seen at 1274 cm^{-1} and benzoate trans-C–H vibration could be observed at 962 cm^{-1}.The nanocomposite showed the Zn–O stretching vibrations at 677 cm^{-1} confirming the presence of ZnO. The disappearance of the band at 962 cm^{-1} of curcumin, and shifting of the band at 881 to 871 cm^{-1} of ZnO could indicate the possible chelation of carbonyl or hydroxyl group of curcumin with Zinc (Moussawi and Patra 2016). Thus, the FTIR spectra indicate the formation of metal-curcumin complex formation (Fig. 1b–d).

The diffraction peaks for ZnO NPs observed at 2θ values are 31.66°, 34.2°, 36.14°, 47.43°, 56.51°, 62.78°, 66.36°, 67.87°, 68.99°, and 72.37° indexed as hexagonal wurtzite phase of ZnO with lattice constants $a = b = 0.324$ nm and $c = 0.521$ nm (JPCDS number: 36-1451) (Zhou et al. 2007). The major XRD diffraction peaks of curcumin were observed at angles 14.5°, 17.2°, 21.17°, 23.47°, and 25.5°. Curcumin exhibited sharp peaks between 10° and 30°, indicating a crystalline structure (Fig. 2). ZnO nanoparticles showed spherical morphology on SEM analysis. SEM micrographs of curcumin are observed in Fig. 3b, and the curcumin consists of particles of various shapes and sizes ranging from 10 to 13 µm. The size range of ZC nanocomposite was found to vary from 200 to 800 nm. This size reduction of curcumin particles is probably due to the nanocurcumin formation and complexation with ZnO NPs during 4 h ultrasonication (Fig. 3c).

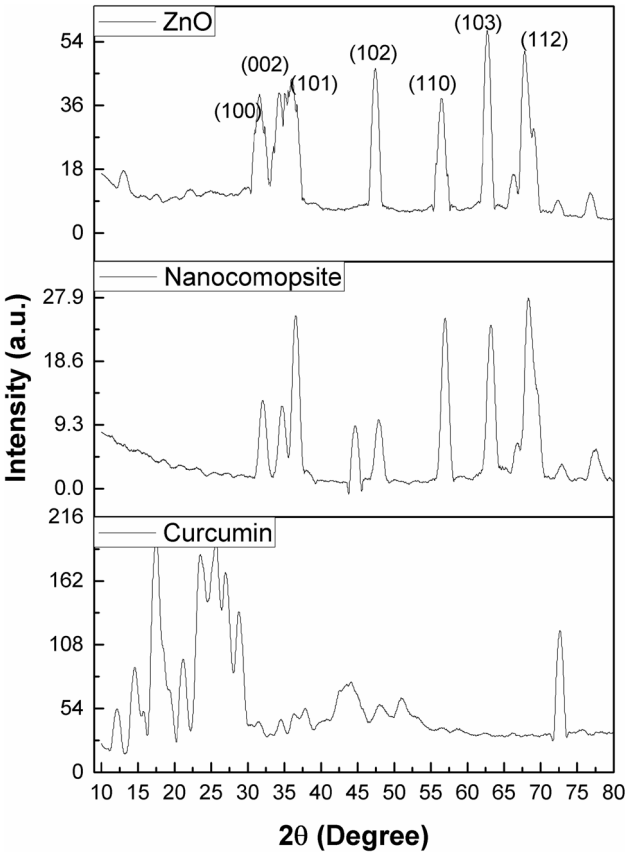

Fig. 2 XRD profiles of ZnO nanoparticles (ZnO), curcumin, and zinc oxide–curcumin nanocomposite (ZC)

Determination of minimum inhibitory concentration (MIC) of nanocomposite against MRCoNS

Ten concentrations of synthesized nanocomposite ranging from 6250 to 12 µg/mL were subjected to broth dilution assay. The lowest concentration which showed no turbidity was visually recorded for all the three isolates. The data were also recorded using spectrophotometry at 600 nm. MIC break points of *S. epidermidis* 107 and *S. hemolyticus* 143 were 195 and 390 µg/mL for *S. saprophyticus* 4 (Fig. 4).

Time kill curve assay of ZC nanocomposite against MRCoNS and fluorescent microscopy analysis

The antibacterial effect of ZC nanocomposite was confirmed by time kill assay. The nanocomposites were used against all the test strains at their respective minimum inhibitory concentrations and OD at 600 nm was measured at specific intervals and plotted (Fig. 5).

Cell viability assay using acridine orange dye revealed that the nanocomposite has a marked effect on clinical isolates. After 24 h of incubation, the treated cells showed red color due to cell death, whereas the viable control showed green fluorescence (Fig. 6).

SEM analysis of treated and untreated bacteria

Surface morphology of nanocomposite treated and untreated bacteria was studied by SEM. The control samples exhibited characteristic grape-like clusters. The treated cells showed no aggregation or clustering and lacked structural integrity. The lack of structural integrity may be due to the cell well damaging effects of nanocomposite material. This indicates the efficacy of nanocomposites as antimicrobial material (Fig. 7).

Surface modification of collagen skin wound dressing with ZC nanocomposite and in vitro analysis of antistaphylococcal activity

Collagen skin wound-dressing membrane was allowed to react with different concentrations of ZC nanocomposite.

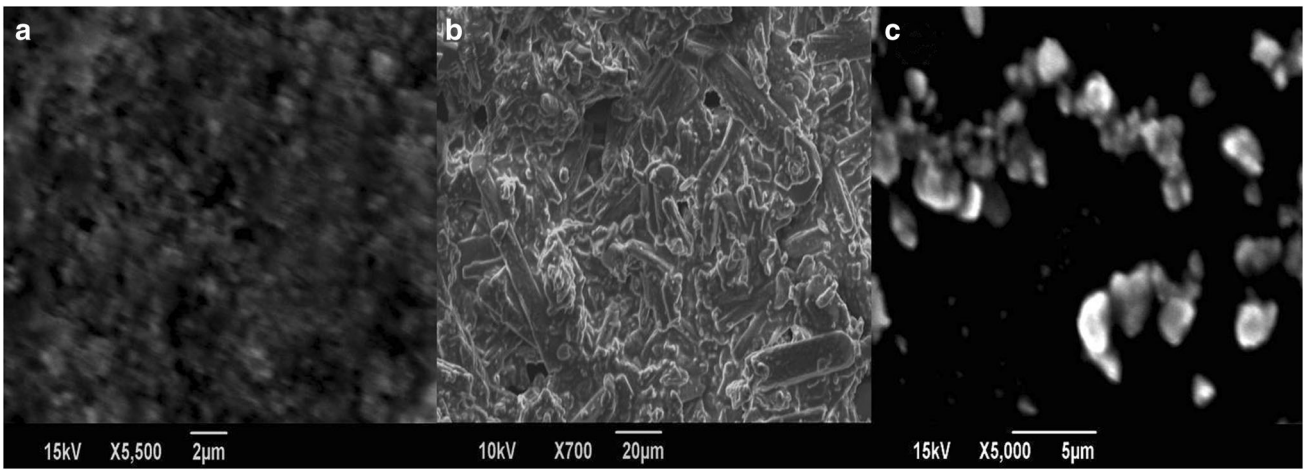

Fig. 3 SEM images of **a** zinc oxide nanoparticles, **b** curcumin, and **c** ZnO–curcumin nanocomposite

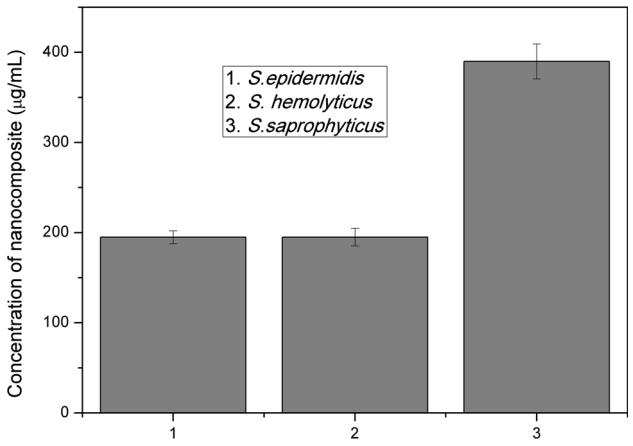

Fig. 4 Minimum inhibitory concentrations of the nanocomposite against (1) *S. epidermidis* 107, (2) *S. hemolyticus* 143, and (3) *S. saprophyticus* 4

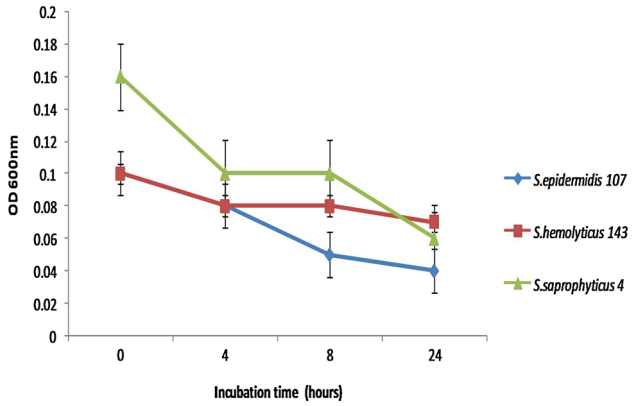

Fig. 5 Time kill assay of MIC concentrations of nanocomposite against MRCoNS

SEM micrographs of treated and untreated dressings indicated the adsorption of ZC nanocomposite onto the collagen membrane (Fig. 8).

On performing the antibacterial assay, *S. epidermidis* and *S. saprophyticus* were found to be susceptible to all the three different concentrations of ZC nanocomposite loaded collagen membrane. The modified membrane showed good clearance zone for *S. hemolyticus* at 10 and 5 mg/mL concentration and a small zone of clearance was observed for 1 mg/mL (Supplementary Table 2, Supplementary Fig. 3).

Discussion

Coagulase-negative Staphylococci have significant clinical importance and approximately 90% of them are resistant to methicillin (John and Harvin 2007; Soumya et al. 2013). Once CoNS breach the skin barrier, they can cause site specific infections (Tan et al. 2006). Involvement of *Staphylococci* in polymicrobial chronic wound infections and related morbidities call for alternatives to the conventional therapeutic strategies (Bradshaw 2011). In the present study, Zinc oxide–curcumin nanocomposite was developed to improve the bioavailability, stability, solubility, and dosage of the individual components to enhance its bioactivity. This could be attributed to the altered physical, chemical, and biological properties of the curcumin–ZnO nanocomposite compared to curcumin or ZnO nanoparticles individually. The presence of the individual components in the synthesized NC was supported by the results of FTIR, XRD, and SEM. The UV spectroscopy and XRD analysis support the surface adherence of curcumin on the ZnO nanoparticles (Dhivya et al. 2015). The SEM investigation revealed the formation of ZnO–curcumin complex after 4 h of water bath sonication and the NCs were found to have dimensions ranging from 200 to 800 nm. (Gopal et al. 2015). The XRD peaks of curcumin disappeared from the nanocomposite which may likely be due to change from crystalline to amorphous form or due to possible even distribution of curcumin crystallites as a thin layer on the ZnO NPs. Most peaks in the ZnO NPs make their appearance in the nanocomposite, but with reduced intensity and a slight shift to the higher angle indicating stresses in the crystal lattice due to reduction in average lattice parameters (Sanphui et al. 2011). The FTIR data are supportive to the chelation of carbonyl or hydroxyl group of curcumin with zinc (Moussawi and Patra 2016). Hence, in the study, a single-step procedure was used for the synthesis of ZnO–curcumin nanocomposites.

Well diffusion assay of ZnO and curcumin against CoNS showed excellent zone of clearance. This was done to confirm that the selected curcumin and ZnO nanoparticles possess antimicrobial properties and have the promises to develop into nanocomposites. Individually, zinc oxide and curcumin have been reported to have excellent antibacterial activity. Curcumin alone was reported to have inhibitory activity against MRSA at MIC value of 125–250 µg/mL. Another study reported the MIC values of curcumin against MSSA and MRSA as 219 and 217 µg/mL, respectively (Gunes et al. 2013). Synergistic effects of curcumin with different antibiotics, ampicillin, oxacillin, and norfloxacin against methicillin-resistant *S. aureus* have been previously reported (Mun et al. 2013). The MIC of ZnO NPs against *S. aureus* was reported to be 1 mg/mL (Reddy et al. 2007). Synergistic combination of ZnO with ciprofloxacin and gentamicin has also been effective in controlling *S. aureus* (Patra et al. 2014; Voicu et al. 2013). A recent study using nanocurcumin and ZnO NPs and curcumin/ZnO nanocomposite against *S. aureus*, *Bacillus subtilis*, *Escherichia coli,* and *Pseudomonas aeruginosa* showed the nanocomposite to have higher efficiency than the pristine ZnO NPs and

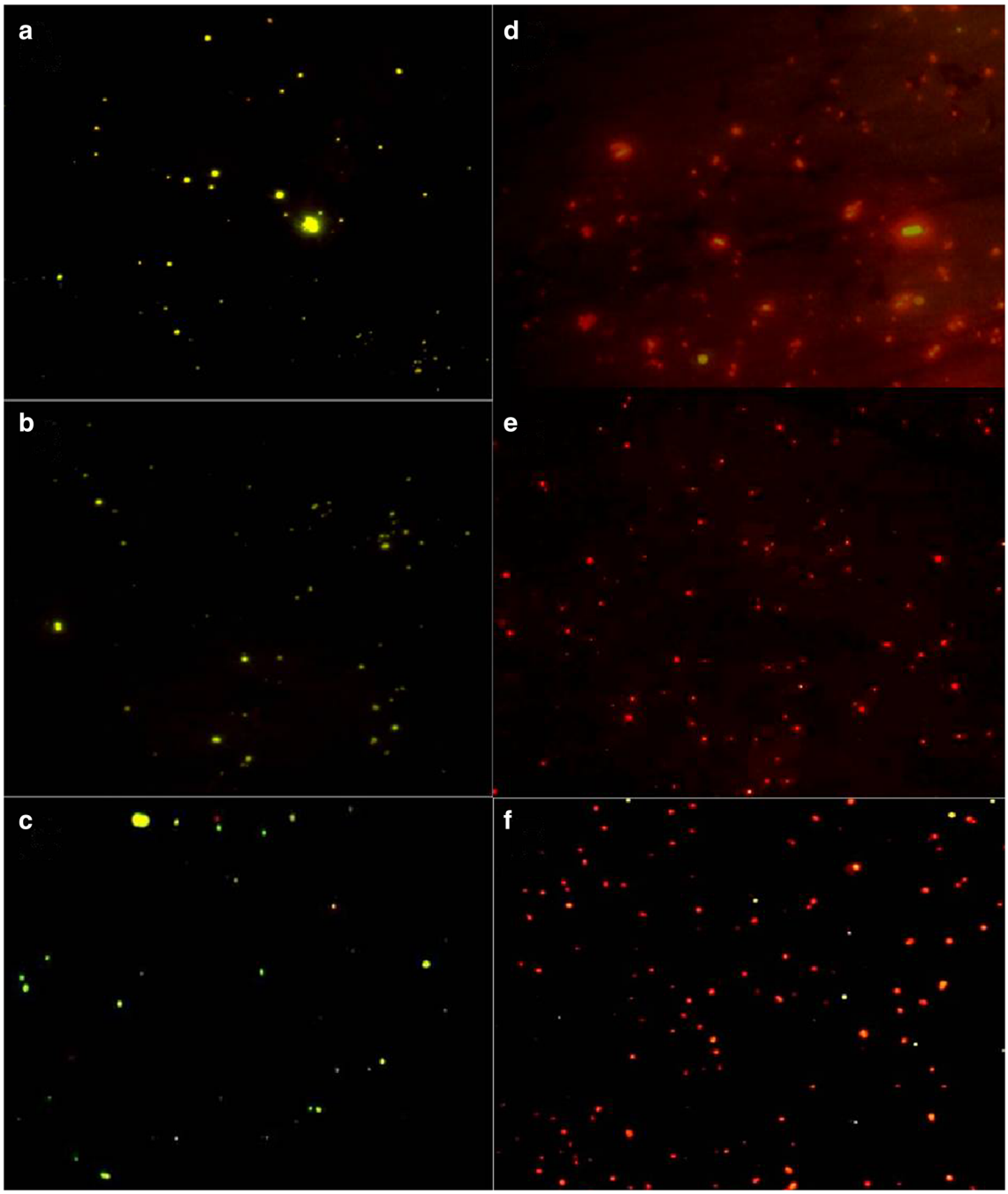

Fig. 6 Cell viability assay by fluorescence microscopy. **a–c** represent the untreated *S. epidermidis* 107, *S. hemolyticus* 143 and *S. saprophyticus* 4 and **d–f** correspond to the treated bacteria at their respective MIC concentrations

nanocurcumin (Dhivya et al. 2015). Most importantly, in the current study, the MIC values of nanocomposites on *S. epidermidis* and *S. hemolyticus* was 195 µg/mL which was much lower than the previous reports of ZnO and curcumin. However, *S. saprophyticus* selected in the study exhibited the MIC value of 390 µg/mL.

The absence of cell clustering and lack of cell integrity in all the CoNS cultures upon nanocomposite treatment are evident from SEM images (Fig. 7). The control organisms showed characteristic clustering of *Staphylococci*. The membrane damaging property of the NC, and thereby, the antistaphylococcal activity can be deduced from the SEM micrographs (Fig. 7) (Babu et al. 2016). Acridine orange staining results from the MIC concentrations of three CoNS were also in accordance with this result. The SEM images from the current and previous studies also point to the

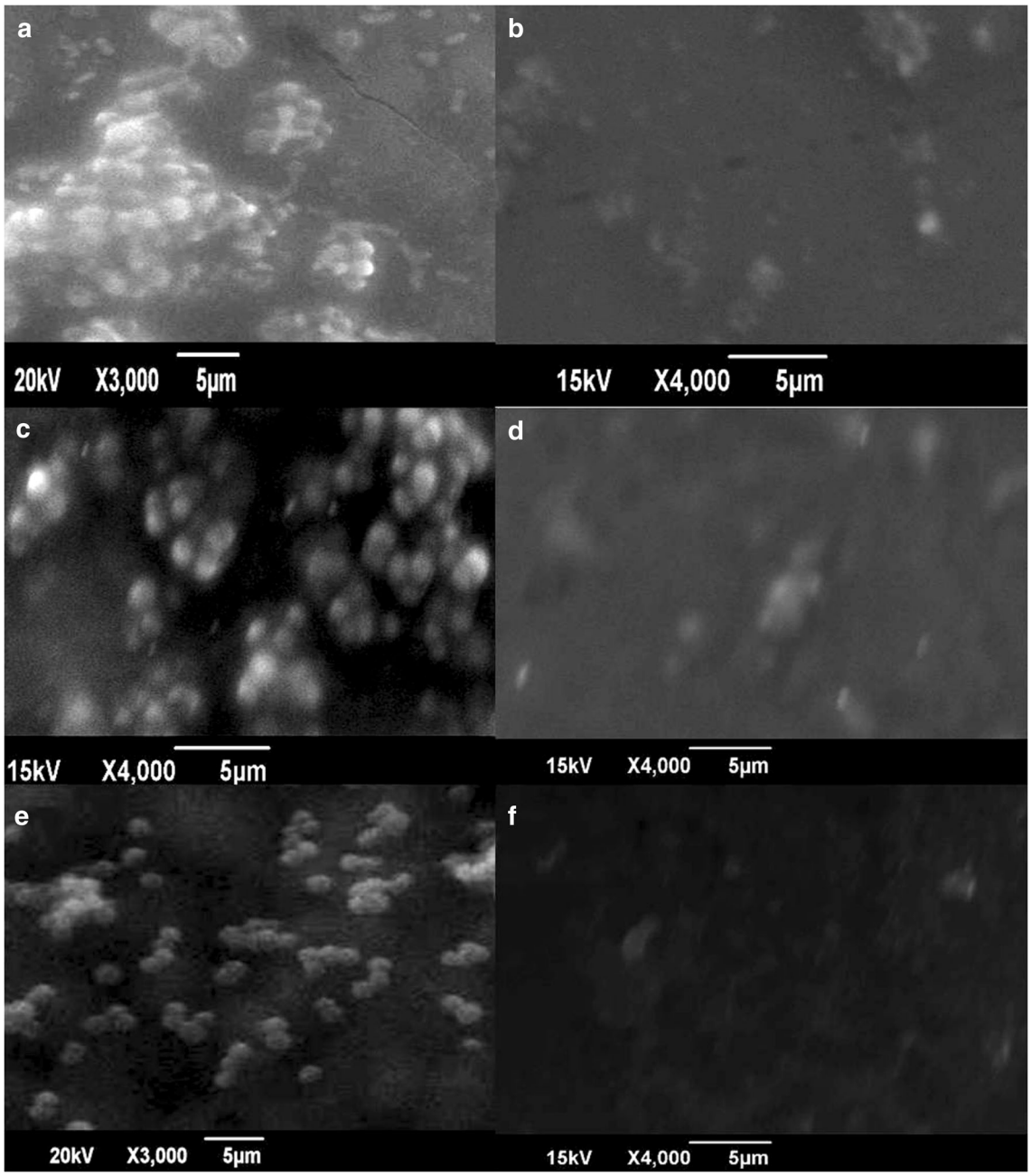

Fig. 7 SEM images **a**, **c,** and **e** represent untreated cultures of *S. epidermidis* 107, *S. hemolyticus* 143, and *S. saprophyticus*, respectively. **b**, **d,** and **f** indicate the MRCoNS treated at 1 mg/mL nanocomposite concentration

membrane damaging properties of the nanocomposite (Lim and Sultana 2016). Curcumin being hydrophobic could bind strongly to the membrane and provide a platform for the more efficient activity of ZnO NPs. Major mechanisms proposed for ZnO NPs include destruction of bacterial cell integrity through the generation of reactive oxygen species and release of antimicrobial Zn^{2+} ions (Augustine et al. 2014; Sirelkhatim et al. 2015). Thus, both the properties of curcumin and zinc oxide could have acted synergistically to result in the pronounced antistaphylococcal effect.

Various studies have been carried out by complexing collagen with curcumin and zinc oxide individually (Guo et al. 2011). However, incorporation of ZnO–curcumin nanocomposite on collagen wound dressing is a novel approach and this has been found to limit the microbial activity with enhanced wound healing effect. Interestingly, the excellent in vitro antistaphylococcal activity shown by nanocomposite loaded collagen skin dressing developed in the study offers promises for its application. The non-toxicity, biodegradability, biocompatibility, weak antigenicity, and ease of remodeling make

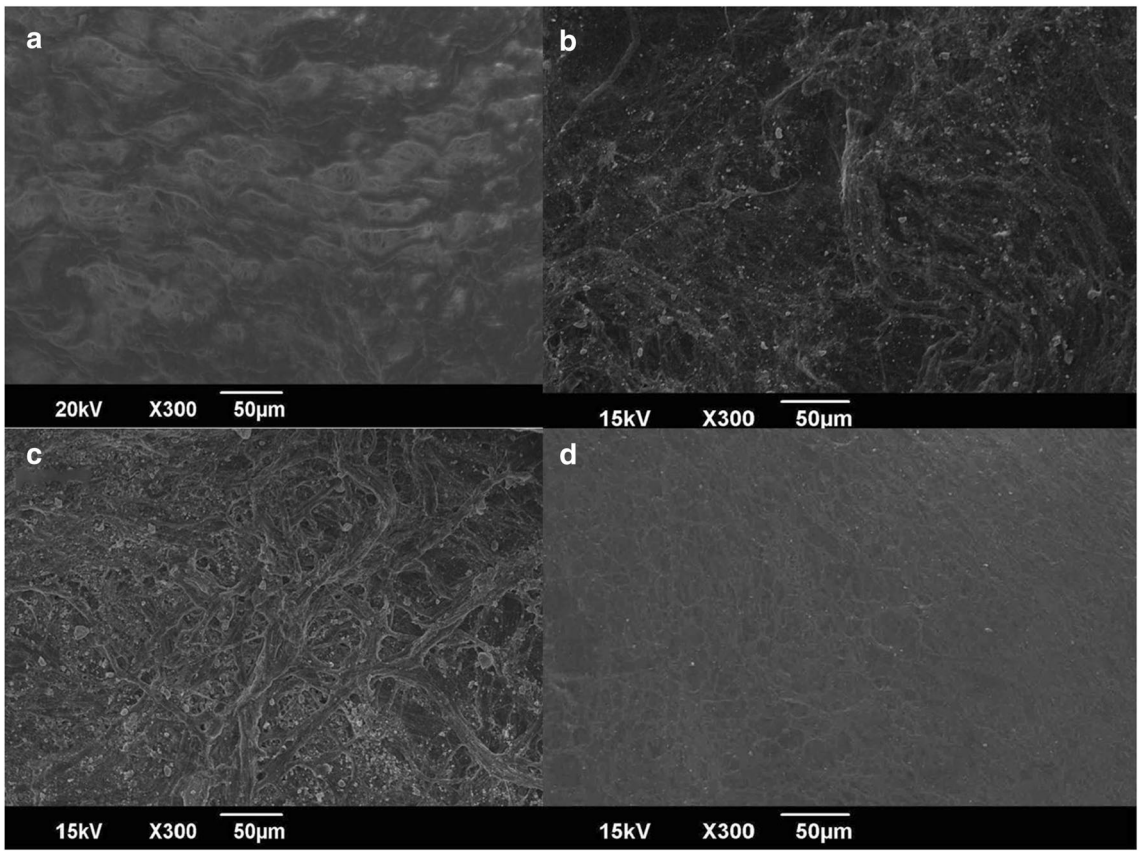

Fig. 8 SEM micrographs of **a** collagen dressing without treatment; **b**, **c,** and **d** represent 10, 5, and 1 mg/mL of ZnO–curcumin nanocomposite-loaded collagen membrane, respectively

collagen an ideal wound dressing for burn wounds and ulcers. The mechanism of interaction present in the nanocomposite-collagen formulation can be mainly through hydrogen bonding and charge interactions, which allow the curcumin to remain in close proximity to the collagen dressing contributing greatly to stabilization of the nanocomposite on the surface of the wound dressing (Esawy et al. 2016). The SEM images of treated collagen dressing showed the adsorbed nanocomposite on the surface of the collagen membrane in a concentration-dependent manner. The ZnO–curcumin nanocomposite embedded on collagen dressing can have faster wound healing and enhanced antimicrobial properties. The advantage with the use of collagen also involves its support to the growth of new tissue by adhering to the walls of the wound and absorbing the wound fluids. Thus, the surface modified collagen membrane as developed in this study can have excellent wound-dressing application (Deepachitra et al. 2014).

ZnO nanoparticles can have toxicity concern at higher concentration. Similarly, the curcumin in spite of its many therapeutic properties has poor bioavailability (Rasmussen et al. 2010). Thus, the current study has effectively harnessed the best of both materials and the resulting NC has been shown to be effective at even very low concentrations. The use of lower concentration of these materials reduces or eliminates its concentration-dependent toxicity.

Conclusions

In conclusion, synthesis and characterization of a novel nanocomposite were carried out in the current study. Properties of zinc oxide–curcumin nanocomposite as effective anti-CoNS agent were analysed. Superior properties such as biosolubility and antimicrobial activity of nanocomposite were obtained when compared with the individual components. The nanocomposite adsorbed collagen skin wound dressing showed remarkable activity against methicillin-resistant *mec* gene harbouring *S. epidermidis*, *S. hemolyticus* and *S. saprophyticus*. Interesting results of this study favor the chance of this antibiotic-free formulation to be used extensively in managing wound infections.

Acknowledgements This work was supported by the Indian Council of Medical Research, Government of India for the funded project on Coagulase-negative staphylococci. We acknowledge Director, School of Chemical Science and School of Pure and Applied Physics,

Mahatma Gandhi University, Kottayam, for the help. We also thank the Department of Biotechnology, Government of India, for DBT RGYI and DBT—MSUB—IPLSARE Programs in School of Biosciences, Mahatma Gandhi University for providing instrumentation facilities. We are grateful to the Dean and laboratory staffs of the MOSC Medical College, Kolenchery.

Compliance with ethical standards

Conflict of interest The authors declare no conflict of interest.

References

Aggarwal BB, Surh Y-J, Shishodia S (2007) The molecular targets and therapeutic uses of curcumin in health and disease. Springer, Heidelberg. doi:10.1007/978-0-387-46401-5

Augustine R, Malik HN, Singhal DK, Mukherjee A, Malakar D, Kalarikkal N, Thomas S (2014) Electrospun polycaprolactone/ZnO nanocomposite membranes as biomaterials with antibacterial and cell adhesion properties. J Polym Res 21:1. doi:10.1007/s10965-013-0347-6

Babu SS, Mathew S, Kalarikkal N, Thomas S (2016) Antimicrobial, antibiofilm, and microbial barrier properties of poly (ε-caprolactone)/cloisite 30B thin films 3. Biotechnology 6:249

Bradshaw CE (2011) An in vitro comparison of the antimicrobial activity of honey, iodine and silver wound dressings. Biosci Horiz 4:61–70. doi:10.1093/biohorizons/hzr008

Deepachitra R, Ramnath V, Sastry TP (2014) Graphene oxide incorporated collagen–fibrin biofilm as a wound dressing material. RSC Adv 4:62717–62727. doi:10.1039/c4ra10150b

Dhivya R, Ranjani J, Rajendhran J, Rajasekaran M, Annaraj J (2015) pH responsive curcumin/ZnO nanocomposite for drug delivery. Adv Mater Lett 6:505–512

Esawy MA, Awad GE, Wahab WAA, Elnashar MM, El-Diwany A, Easa SM, Fawkia M (2016) Immobilization of halophilic *Aspergillus awamori* EM66 exochitinase on grafted k-carrageenan-alginate beads 3. Biotechnology 6:29

Gopal J, Muthu M, Chun SC (2015) One-step, ultrasonication-mobilized, solvent-free extraction/synthesis of nanocurcumin from turmeric. RSC Adv 5:48391–48398. doi:10.1039/c5ra06002h

Gunes H, Gulen D, Mutlu R, Gumus A, Tas T, Topkaya AE (2013) Antibacterial effects of curcumin: an in vitro minimum inhibitory concentration study. Toxicol Ind Health 32:246–250. doi:10.1177/0748233713498458

Guo G et al (2011) Preparation of curcumin loaded poly (ε-caprolactone)-poly (ethylene glycol)-poly (ε-caprolactone) nanofibers and their in vitro antitumor activity against Glioma 9L cells. Nanoscale 3:3825–3832

Jin T, Sun D, Su JY, Zhang H, Sue HJ (2009) Antimicrobial efficacy of zinc oxide quantum dots against *Listeria monocytogenes*, Salmonella Enteritidis, and *Escherichia coli* O157:H7. J Food Sci 74:M46–M52. doi:10.1111/j.1750-3841.2008.01013.x

John JF, Harvin AM (2007) History and evolution of antibiotic resistance in coagulase-negative staphylococci: Susceptibility profiles of new anti-staphylococcal agents. Ther Clin Risk Manag 3:1143

Kumar H, Rani R (2013) Structural and optical characterization of ZnO nanoparticles synthesized by microemulsion route. Int Lett Chem Phys Astron 14:26–36

Lim MM, Sultana N (2016) In vitro cytotoxicity and antibacterial activity of silver-coated electrospun polycaprolactone/gelatine nanofibrous scaffolds 3. Biotechnology 6:211

Mei L, Wang Y, Tong A, Guo G (2016) Facile electrospinning of an efficient drug delivery system. Expert Opin Drug Deliv 13:741–753

Mohanty C, Das M, Sahoo SK (2012) Sustained wound healing activity of curcumin loaded oleic acid based polymeric bandage in a rat model. Mol Pharma 9:2801–2811. doi:10.1021/mp300075u

Moussawi RN, Patra D (2016) Modification of nanostructured ZnO surfaces with curcumin: fluorescence-based sensing for arsenic and improving arsenic removal by ZnO. RSC Adv 6:17256–17268

Mun S-H et al (2013) Synergistic antibacterial effect of curcumin against methicillin-resistant *Staphylococcus aureus*. Phytomedicine 20:714–718. doi:10.1016/j.phymed.2013.02.006

Mun S-H et al (2014) Curcumin reverse methicillin resistance in *Staphylococcus aureus*. Molecules 19:18283–18295. doi:10.3390/molecules191118283

Panchatcharam M, Miriyala S, Gayathri VS, Suguna L (2006) Curcumin improves wound healing by modulating collagen and decreasing reactive oxygen species. Mol Cell Biochem 290:87–96

Patra P, Mitra S, Debnath N, Pramanik P, Goswami A (2014) Ciprofloxacin conjugated zinc oxide nanoparticle: a camouflage towards multidrug resistant bacteria. Bull Mater Sci 37:199–206. doi:10.1007/s12034-014-0637-6

Piette A, Verschraegen G (2009) Role of coagulase-negative staphylococci in human disease. Vet Microbiol 134:45–54. doi:10.1016/j.vetmic.2008.09.009

Rasmussen JW, Martinez E, Louka P, Wingett DG (2010) Zinc oxide nanoparticles for selective destruction of tumor cells and potential for drug delivery applications. Expert Opin Drug Deli 7:1063–1077

Reddy KM, Feris K, Bell J, Wingett DG, Hanley C, Punnoose A (2007) Selective toxicity of zinc oxide nanoparticles to prokaryotic and eukaryotic systems. Appl Phys Lett 90:213902. doi:10.1063/1.2742324

Sanphui P, Goud NR, Khandavilli UR, Bhanoth S, Nangia A (2011) New polymorphs of curcumin. Chem Commun 47:5013–5015

Sirelkhatim A et al (2015) Review on zinc oxide nanoparticles: antibacterial activity and toxicity mechanism. Nano Micro Lett 7:219–242. doi:10.1007/s40820-015-0040-x

Soumya KR, Thomas SA, Sugathan S, Mathew J, Radhakrishnan EK (2013) Antibiotic susceptibility and multiplex PCR analysis of coagulase negative staphylococci isolated from laboratory workers. Int J Curr Microbiol Appl Sci 2:266–272

Soumya KR, Sugathan S, Mathew J, Radhakrishnan E (2016) Studies on coexistence of mec gene, IS256 and novel sasX gene among human clinical coagulase-negative staphylococci 3. Biotechnology 6:233

Tan TY, Ng SY, Ng WX (2006) Clinical significance of coagulase-negative staphylococci recovered from nonsterile sites. J Clin Microbiol 44:3413–3414. doi:10.1128/jcm.00757-06

Thomas R, Soumya KR, Mathew J, Radhakrishnan EK (2015) Inhibitory effect of silver nanoparticle fabricated urinary catheter on colonization efficiency of coagulase negative staphylococci. J Photochem Photobiol B 149:68–77. doi:10.1016/j.jphotobiol.2015.04.034

Tocco I, Zavan B, Bassetto F, Vindigni V (2012) Nanotechnology-based therapies for skin wound regeneration. J Nanomater 2012:1–11. doi:10.1155/2012/714134

Voicu G, Oprea O, Vasile B, Andronescu E (2013) Antibacterial activity of zinc oxide-gentamicin hybrid material. Dig J Nanomater Biostruct (DJNB) 8(3):1191–1203

Zhou J, Zhao F, Wang Y, Zhang Y, Yang L (2007) Size-controlled synthesis of ZnO nanoparticles and their photoluminescence properties. J Lumin 122–123:195–197. doi:10.1016/j.jlumin.2006.01.089